2023

Pathogen transmission by aerosol particles. — A positive outcome of the COVID-19 pandemic was the focus on research aimed at understanding the mechanisms of epidemic spread and, with it, the recognition and research into the role of aerosols in the transmission of infections. The transmission mechanisms of pathogens have been investigated in hospital settings and the laboratory.

At the Pulmonology Hospital of Törökbálint and the Department of Pulmonology of Semmelweis University, in addition to monitoring airborne particles, size-fractionated samples were collected using a cascade impactor for further analysis. The focus of our investigations was micron and submicron particles. Optical particle counters measured size distributions and concentrations from 250 nm to 32 µm with a high temporal resolution and 8-h impactor sampling was performed in the range of 70 nm to 10 µm in 9 size ranges on gelatin filters during the alpha and delta variant periods. The large number (152) of size-fractionated samples allowed statistical analysis of SARS-CoV-2 RNA copies over a wide range of aerosol particle sizes. Our results showed that SARS-CoV-2 RNA is most likely found in particles with aerodynamic diameters of 0.5–4 µm but also ultrafine particles. The correlation analysis of particulate matter (PM) and RNA copies highlighted the importance of indoor medical activity. It was found that the daily maximum increase in PM mass concentration correlated most strongly with the RNA number concentration of SARS-CoV-2 in the corresponding size fractions. Our results suggest that particle resuspension from surrounding surfaces is an important source of SARS-CoV-2 RNA present in the air of hospital rooms.

In our laboratory studies, we measured the size distribution and concentration of exhaled aerosol particles and their variation over time during normal speech. In addition, the filtering efficiency of three commonly used face masks (FFP2, surgical and 2-layer cotton masks) was investigated under real conditions. A series of experiments were conducted with 28 participants in a specially designed and constructed cabin providing a cleanroom environment (Fig.1.). A Lasair III 110 cleanroom aerosol spectrometer measured size distributions of the emitted particles with high time resolution (6 s) in the 0.1–5 μm size range (Fig.1.). Our results showed that, although the shape of the size distribution curves was similar in all cases, the number of particles emitted differed significantly between individuals and generally decreased to different extents during normal speech. Based on high temporal resolution measurements, we showed that the number concentration of emitted submicron particles varied significantly as a function of speech volume. The FFP2 and the surgical masks showed robust performance under real conditions, even for the smallest size ranges tested, with a filtering efficiency of approximately 80%. In contrast, textile masks performed less favourably, with an average filtration efficiency of around 50-60%. Our results show that while the filtering efficiency of FFP2 masks exceeds that of surgical masks, the difference is insignificant in everyday wear.

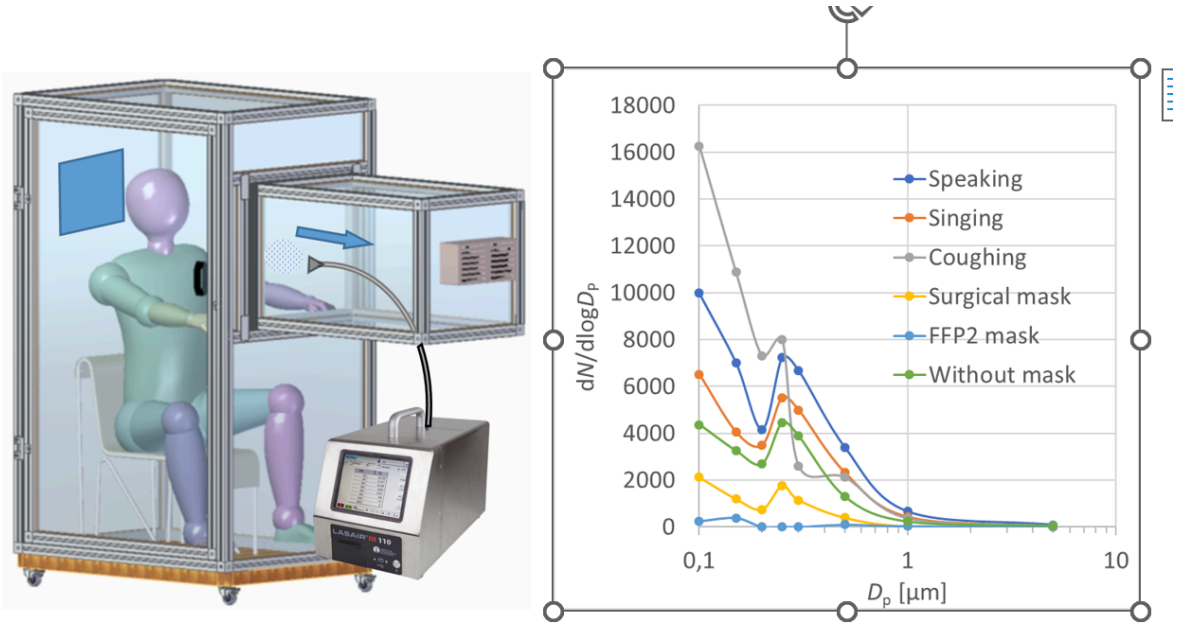

Figure 1. The measurement set-up (left panel) and typical size distributions of emitted particles during different

activities (right panel). A weak laminar flow was maintained in the cabin through a ULPA filter to achieve cleanroom conditions. For the mask tests, subjects performed the same activity (counting from 1 to 100).

Nanoparticle emission during a 3D metal printing process — Three different particle fractions were identified in the sampled air during 3D metal printing. Significant aerosol formation was observed in the ultrafine size range, where the elemental composition of the particles changed compared to the powder used for construction (Fig.2.). The fraction in the submicron range consists of spherical particles with a slightly different composition from the starting powder and was probably formed during the laser interaction from the starting material. The particle fraction above one micron is derived from the starting powder, it was mechanically detached from the initial powder in the powder feeder.

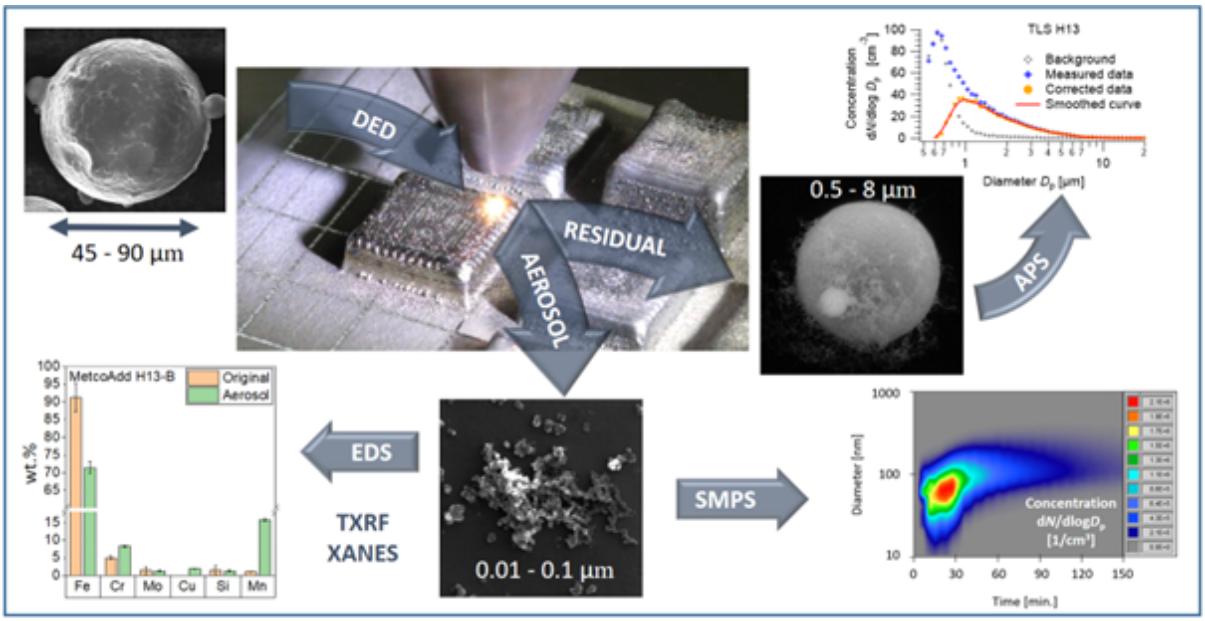

Figure 2. Characterization of particle fractions generated during 3D metal printing.

2022

Pathogen transmission by aerosol particles — During the COVID-19 pandemic, pulmonary function tests and bronchoscopy, known to emit particles, were considered high risk for virus transmission. However, these tests are essential in selecting appropriate therapy for lung diseases. Therefore, respiratory function and bronchoscopy laboratory measurements were designed to quantify patients' particulate emissions, which can be used to estimate viral load and assess the associated risks. The measurements were performed in a real-life environment during patient examinations. Optical particle counters measured emitted particle concentrations and size distributions, and the viral load was determined by model calculations. Our results indicate that the concentration and size distribution of particles emitted by patients during the tests (Fig.1.) are similar to those released into the air during normal speech or other similar activities and therefore do not represent a significant viral burden for the healthcare personnel. These tests can therefore be carried out following standard protection protocols, and there is no justification for not carrying them out.

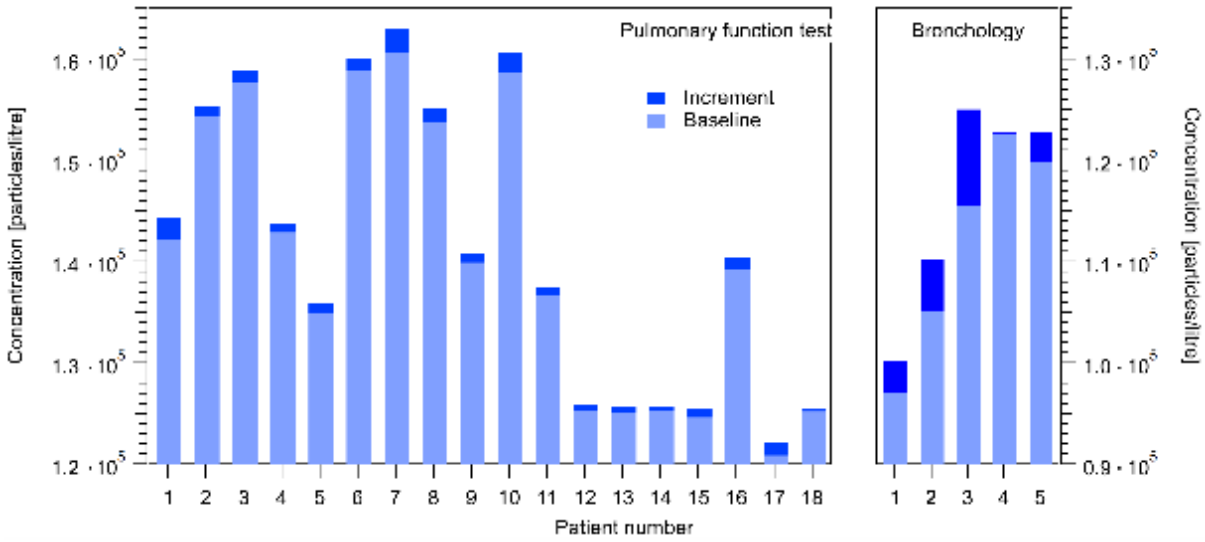

Figure 1. Results of measurements taken during pulmonary function and bronchoscopy tests.

Aerosol drug delivery/deposition in human lungs — Aerosol medicines are most commonly used for the effective local treatment of various respiratory diseases. The use of nano-sized active ingredients results in higher bioavailability due to their larger specific surface area. Extra fine dry powder drugs reach smaller airways, further improving therapeutic efficacy. In collaboration with the Institute of Pharmaceutical Technology and Regulatory Affairs at the University of Szeged, we aimed to determine the airway deposition properties of newly synthesised drug substances under real conditions: using a realistic respiratory waveform and geometry that takes into account the effect of the upper airways. Based on our results, we found that the distributions measured by the optical method are in agreement with the results of impactor measurements standardised in the pharmaceutical industry (Fig.2.). In both cases, it can be concluded that the powders can reach the target area, the deeper part of the lung, and thus treat the inflammation and infections present there.

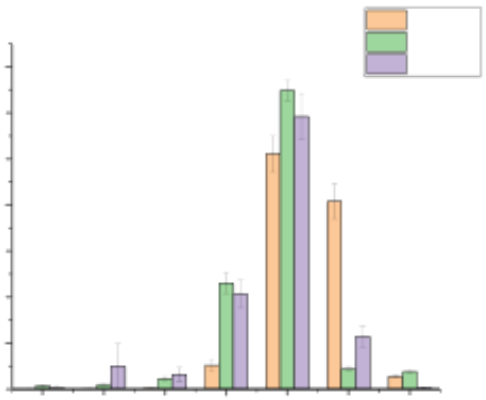

Figure 2. Comparison of the drug distribution of meloxicam-containing formulations with the size distributions measured by APS. APS-C gives the distribution by number, APS-M gives the distribution by volume (mass) projected onto the ACI impactor plates.

2021

Pathogen transmission by aerosol particles — Several pathogens enter a host via airway and lung epithelial cells, including SARS-CoV-2. Virulence, host factors, and accessibility are the key determinants of microbial lung infections. Hospital-acquired infections represent a global health care problem. Our research aimed to gain a better insight into airborne particle-associated ways of disease transmission and prevention. Health care personnel and patient activity associated changes in particle size and concentration in the position of an imaginary roommate heads position in a hospital bedroom with a single bedridden COVID-19 patient was monitored with an optical particle counter. Type and duration, as well as the number of health care personnel, were recorded. Concentration changes associated with specific activities were determined, and airway deposition

modeling was performed using these data. Thirty-one activities were recorded, and six representatives were selected for deposition modeling, including patient's activities (coughing, movements, etc.), monitoring, and patient care (e.g., drug administration, temperature measurement, blood sampling, medications, diagnostic test, bedding). The increase in particle concentration of all sizes was very sensitive to the type of activity and ventilation (Fig.1.). A larger particle concentration increase was associated with the health care professional number ($r=0.66$; $p<0.05$) and the duration of activity ($r=0.82$; $p<0.05$). The number and mass of inhaled particles deposited on the unit surface were 1.5×10^5 and 2.2×10^7 times higher in the upper airways, and a significant amount was deposited in the bronchial airways and acinar region. Our data confirm that even short periods of health care personnel activity results in a severe disturbance of micron and submicron-sized airborne particles, which deposit in different parts of the lungs of the adjacent bed patient. Hospital-acquired airway and lung infections might develop differently according to the intensity and frequency of a given activity-associated particle disturbance, especially highlighting possible multidrug-resistant pathogen transmissions.

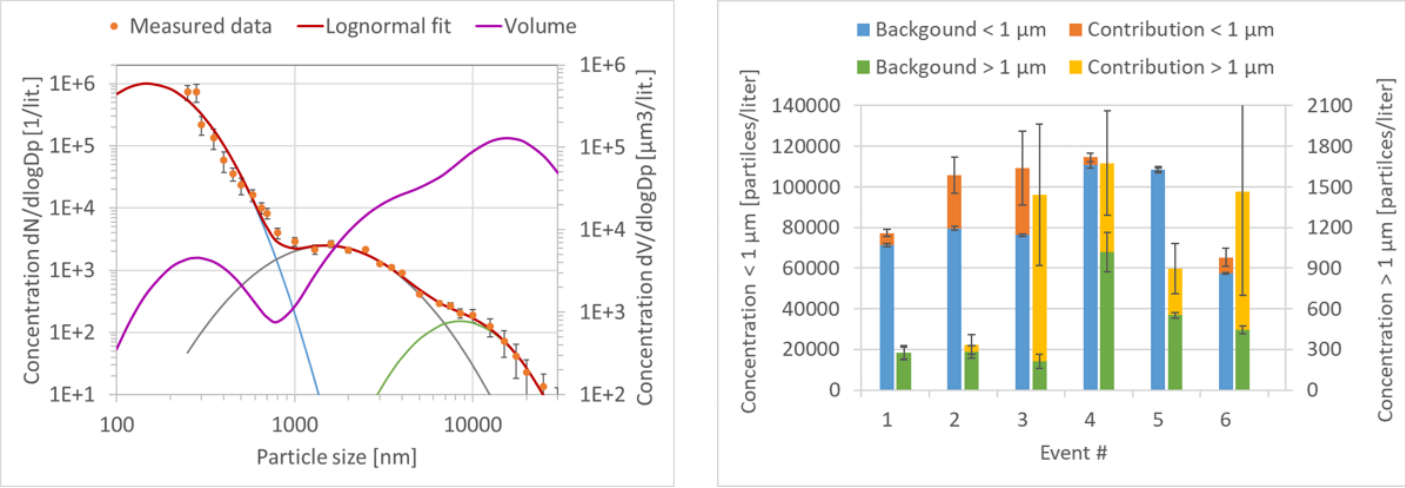

Figure 1. Measured size distribution (left graph) and the contribution of the six selected events to the background concentration (right graph) [1].

Nanoparticle formation and emission during intense laser-matter interactions — In this year, we focused on the H13-type hot work tool steel. The physical and chemical properties of the two kinds of H13 steel powders and aerosols formed in the laser cladding process were compared. During the cladding process, the measured number size distribution follows the lognormal distribution with a peak value at 70 nm, and the peak value of the calculated mass or volume size distribution is at 200 nm. The calculated size distribution of the iron (Fe), which is the balance in the composition of the H13 types steels, show a remarkable agreement with the double peak volume size distributions calculated from the number size distributions measured by the two aerosol measuring instruments.

Development of new know-how to produce special laser optical elements – I. Zero dispersion, minimal absorption damping filters (O.D. = 0.5, 1 or 2) in the wavelength range 500-1100 nm; II. Coatings for low transmission loss windows and focusing lenses for 1030 nm femtosecond lasers; III. Laser mirrors with R> 99.95% reflectance for 3350 nm laser wavelength; IV. Zero dispersion metal-dielectric laser mirrors with R> 99% reflectance for different spectral ranges.

2020

Aerosol deposition in human lungs – The new coronavirus disease is thought to spread mainly by droplet infection when an infected person coughs, sneezes, or talks and a bystander person inhale the droplets containing the pathogen of COVID-19. We applied the Stochastic Lung Deposition Model to quantify the deposition distribution of the droplets and aerosol particles containing SARS-CoV-2 (Centre for Energy Research). It was found that the probability of direct infection of the acinar airways due to inhalation of particles emitted by a bystander person is very low. As the number of viruses deposited in the extrathoracic airways is about seven times higher than in the acinar airways, we concluded that COVID-19 pneumonia must be preceded by SARS-CoV-2 infection of the upper airways in most cases. [1]

Particle size distribution, breathing parameters, and viral loads were taken from the literature. We assumed that the virus distribution is homogenous in the initial throat swab sample and that the number of viruses in a particle is proportional to its mass. In this case, the probability that a particle contains at least one RNA copy of the virus can be calculated assuming Poisson distribution. Figure 1 shows the average number of RNA copies per particle and the probability that a particle contains at least one RNA copy of the virus as the function of particle size.

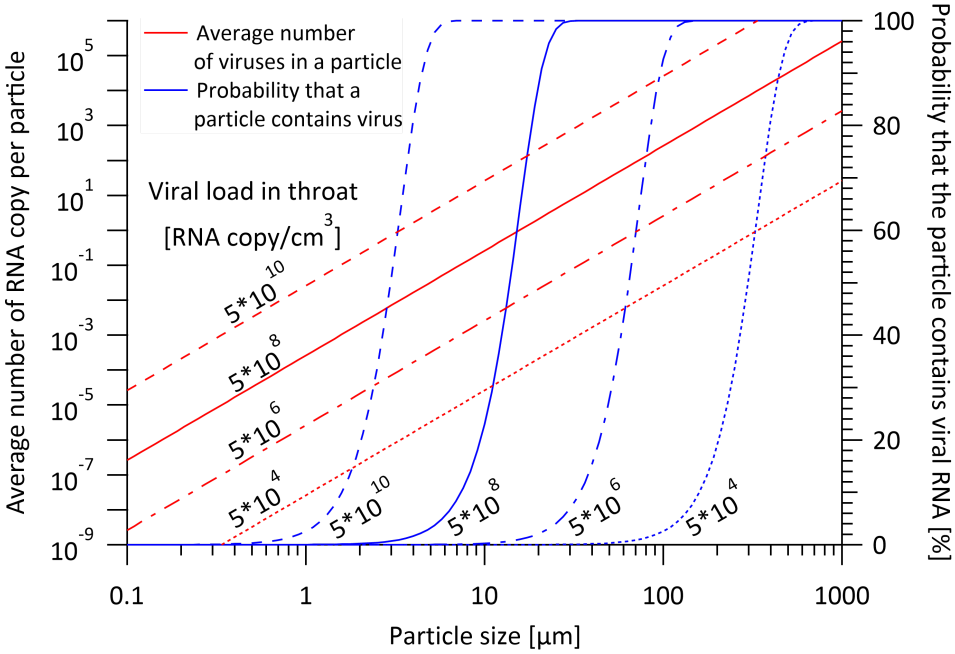

Figure 1. *The average number of RNA copies of the virus in one particle (left axis and red lines) and the probability that a particle contains at least one RNA copy (right axis and blue lines) as the function of particle size in case of different initial viral loads (in RNA copy per cm3) in the throat.*

Nanoparticle formation and emission during intense laser-matter interactions – We have characterized the emitted aerosol particles with respect to their dominating diameter range, morphology, elemental composition, and oxidation state of selected metals (Cr, Mn, Fe, and Ni), aiming to describe their enrichment/depletion and oxidation compared to the original feedstock powder. Together with an SMPS total and size-fractionated aerosol samples were collected by a filter pack and a cascade impactor, respectively. Morphology and elemental composition of the particles were investigated by scanning electron microscopy (SEM) and energy dispersive spectroscopy (EDS). Collective elemental analysis of the aerosol particles was performed by total-reflection and microscopic X-ray fluorescence methods (TXRF, *µ*XRF). The oxidation state of selected metals in the aerosol particles was studied non-destructively using the X-ray absorption near-edge structure method (XANES) (Figure 2). AM machines can generate hazardous particles, which can raise occupational health issues for the operators of the machines. Furthermore, the nanoparticles can influence the efficiency of the laser during operation. We studied the effects of the different parameters on the properties of the created objects. The studied parameters were laser power, beam shape, quality, focusing, moving parameters, building strategies, parameters of the hatching and the perimeter, composition of the used powder, finishing strategies, shield gas flowrate, etc.

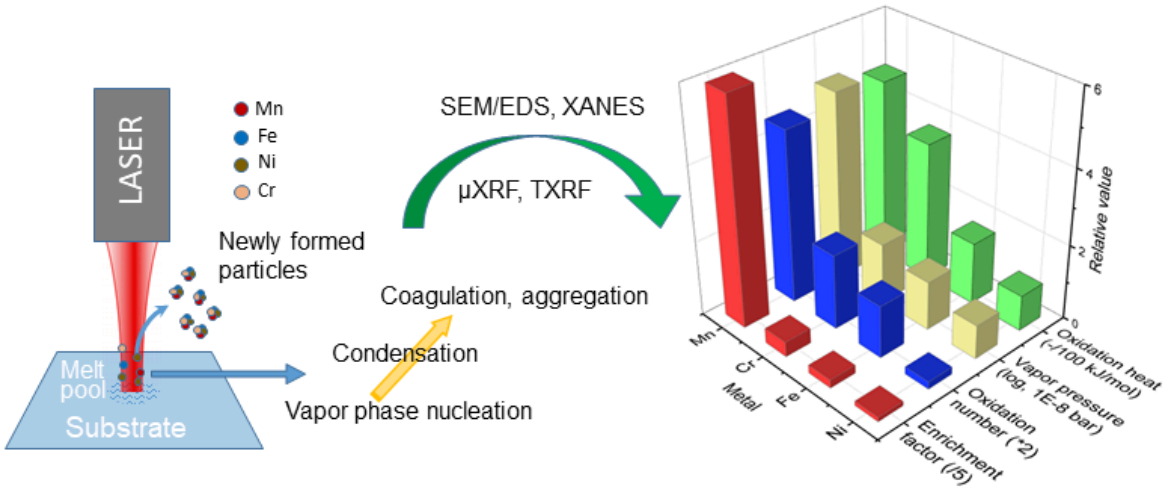

Figure 2. *Temporal evolution of the measured size distribution of the particles emitted during a laser cladding*

process. The color code represents number concentrations [1/cm^3].

Measured size distributions and aerosol properties are in line with available literature data. Particle formation starts from below 10 nanometers, and the average particle size was between 50 and 60 nm during the process. When the cladding process was finished, the average size increased to around 100 nm within 30 minutes. (Figure 3).

The chemical composition of the released aerosol particles can be characterized by significant amounts of Fe, Cr, Mn, and Ni, where Ni, Cr, and Mn are toxic metals. An important feature of the ultrafine metal oxide particles is the Mn enrichment, which, together with their large amount, increase their toxic potential as a function of decreasing particle size.

Development of new know-how to produce special laser optical elements – I. Zero dispersion, minimal absorption damping filters (O.D. = 0.5, 1 or 2) in the wavelength range 500-1100 nm; II. Coatings for low transmission loss windows and focusing lenses for 1030 nm femtosecond lasers; III. Laser mirrors with R> 99.95% reflectance for 3350 nm laser wavelength; IV. Zero dispersion metal-dielectric laser mirrors with R> 99% reflectance for different spectral ranges.

2019

Aerosol drug delivery/deposition in human lungs. – Experimental and numerical simulation methods were used to determine the efficiency of aerosol drugs, and a new method were proposed to enhance the efficiency of personalized therapies and reduce side effects. We studied the effects of the turbulences generated by the inhalation devices on the measured breathing parameters during standard spirometry. The observed turbulences may lead to false results during the measurement of the peak inhalation flow rate which may cause problems in the selection of the proper inhalation device used for the treatment of pulmonary diseases.

Development of the technology based on 3D metal printing. – Laser cladding by powder injection is a widely used technique in industrial applications such as additive manufacturing, parts repair, surface coating, etc. The powder used in laser cladding is normally a metallic alloy, and is injected into the system by coaxial or lateral nozzles. While the focused intense laser beam creates a melt pool on the surface of a substrate, the metallic powder stream also interacts with the laser and the particles deposit into the melt pool. Moving the substrate allows the melt pool to solidify and thus produces a track of solid metal which form a 3D object at the end (Fig.1.).

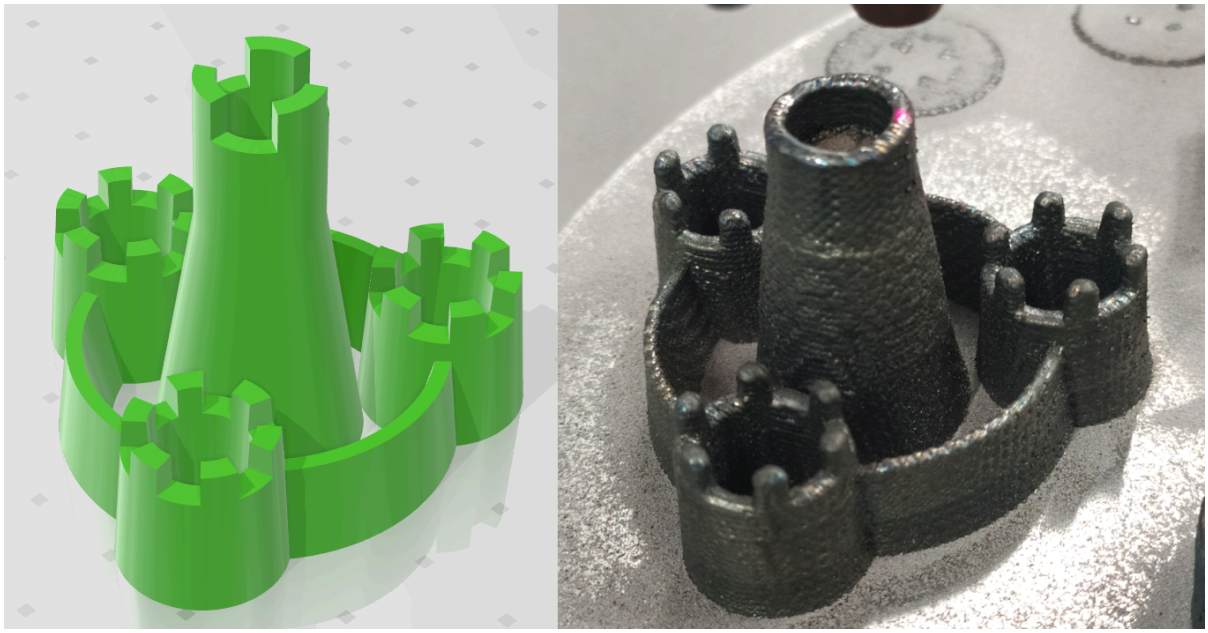

Figure 1. *3D printed object (during the printing process) with a laser-welding machine utilizing the direct energy deposition method.*

Demo cubes were built from Ni-based metallic powder by a laser-welding machine utilizing the direct energy deposition method onto a stainless steel substrate. We studied the effects of the different parameters on the properties the created objects (Fig.2.). The studied parameters were laser power, beam shape and quality,

focusing, moving parameters, building strategies, parameters of the hatching and the perimeter, composition of the used powder, finishing strategies, shield gas flowrate, etc.

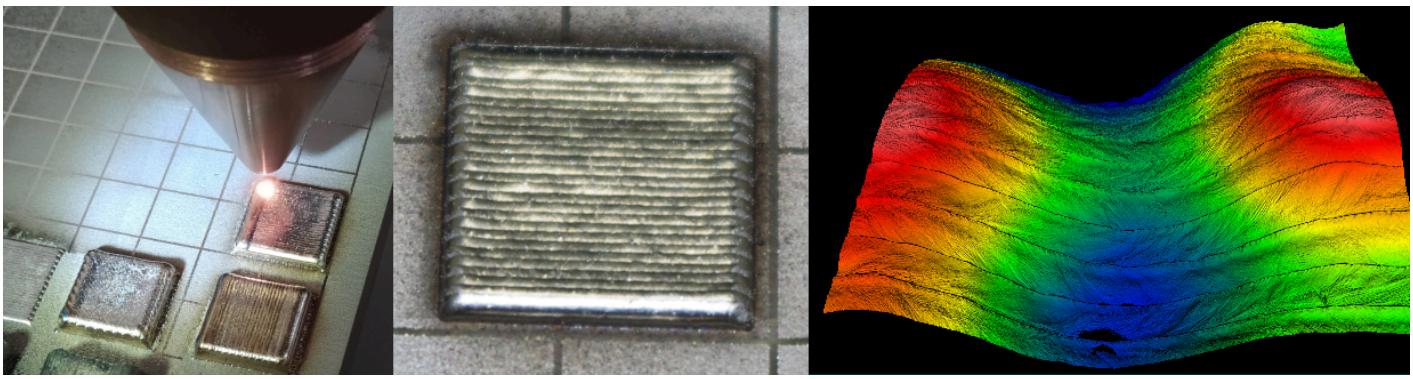

Figure 2. *Building process of a demo cube by laser cladding with metallic powder (left), a typical demo cube which was built to study the effects of the building parameters (middle), and a reconstructed surface with the Zygo NewViewTM 7100 interferometric surface profiler (right).*

Nanoparticle formation and emission during intense laser-matter interactions. – We have studied the properties of the generated ultrafine smoke during the laser-welding processes. Different instruments were utilized to retrieve the properties of the released aerosol particles.

Particle formation during the process starts from below 10 nm, and the average particle size was between 50 and 60 nm. When the cladding process was finished, the average size increased to around 100 nm within 30 minutes period (Fig.3.). The generated smoke contains a considerable amount of ultrafine particles, where the filtration requires special techniques.

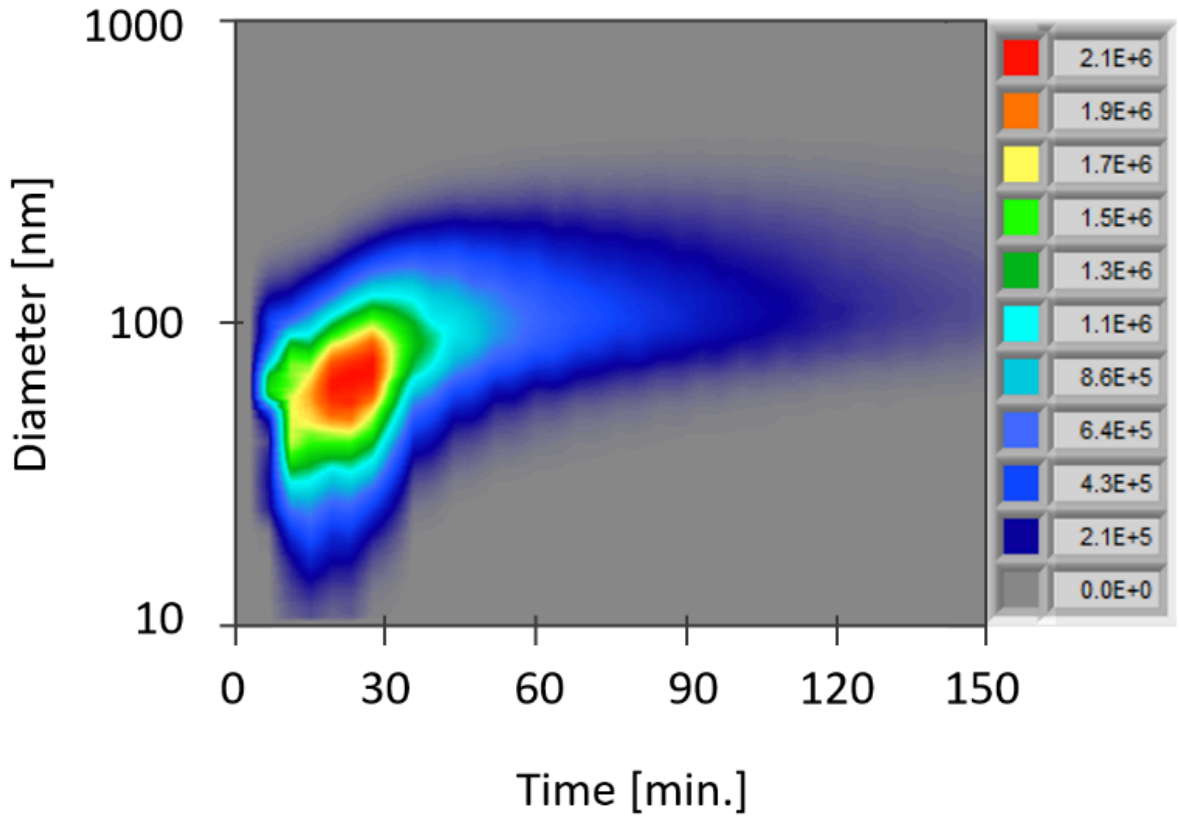

Figure 3. *Temporal evolution of the measured size distribution of the particles emitted during a laser cladding process. The colour code represents number concentrations [1/cm3].*

Health effects, occupational health – The health effects of the plume, which is released during 3D metal printing processes, were investigated by means of optical, electrostatic, inertial and spectroscopic techniques. While the typical size of metal powders, produced by inert gas atomization, span from 10 to 150 μm, it may contain alveolar as well as inhalable dust fractions and contain hazardous elements. We observed a considerable amount of newly formed aerosol particles in the plume with a size mainly below 1 μm. The fraction of the inhaled aerosol particles, which deposits in the lung, steeply increases with decreasing size in the ultrafine region, which may lead to occupational health problems.

Originally the 718G metal powder has a particle size range between 45 and 90 μm with mostly spherical shape. Fig. 4. shows the average elemental composition of the original powder. During the welding process the mass size distribution of the released particles shows a pronounced peak between 100 and 200 nm. The Ni-to-Cr ratio changed from approximately 2 (original metal powder) to around 0.67 (aerosol particles). Although Mn was not detected in the original powder, significant amount was released during laser welding. 95% of the Cr and 89% of the Ni was found in particles between 70 and 180 nm.

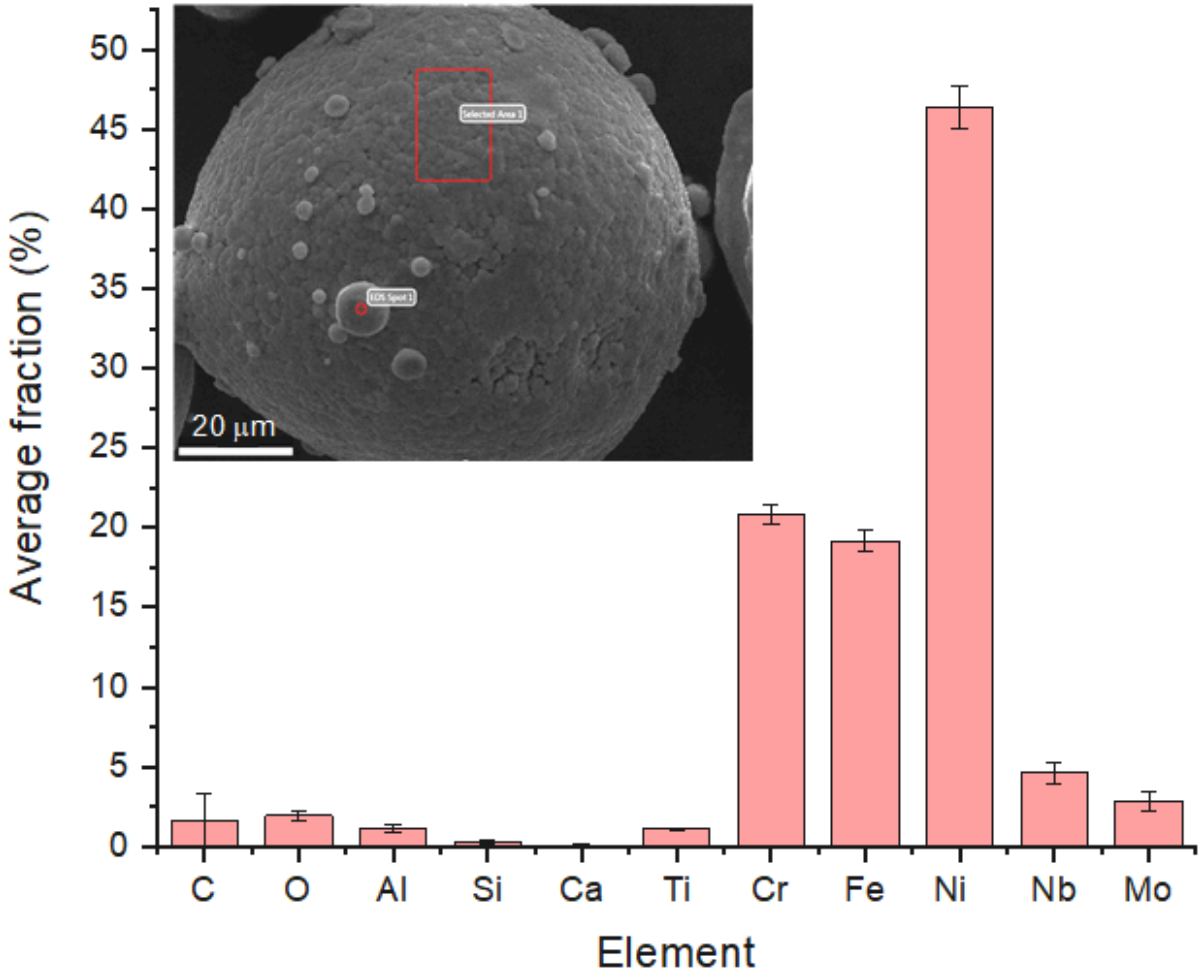

Figure 4. *Elemental composition of the MetcoAdd 718G metallic powder detected with Energy Dispersive Spectroscopy*

2018

Aerosol drug delivery/deposition in human lungs – In vitro experimental and in silico numerical simulation methods were used for the determination of the deposition distribution and deposition efficiency of aerosol drugs from pressurized metered dose inhalers and dry powder inhalers (widely utilized in the therapy of chronic pulmonary diseases) as a function of standard breathing parameters. The mass median aerodynamic diameter of the released particles was determined for different idealized inhalation waveforms, directly from the inhaler and after a realistic upper airway model. We found that the mass median aerodynamic diameter varies by a factor of 2 and decreases with increasing peak inspiratory flow and inhaled volume. It was measured to be approximately 10% lower after the upper airway. The stochastic lung deposition model was used to calculate the lung deposition of the medicament with each inhalation profile, taking into account the measured size distribution. We determined the minimum required inhalation flow for the examined dry powder inhalers for an acceptable level of lung deposition dose. Above 60 L/min peak inspiratory flow the lung deposition increases above 50%, which may support a sufficient therapy. Our measurements showed that the length of the inhalation does not influence the lung deposition dose, peak inspiratory flow and inhaled volume are much more relevant factors. We presented a map of the deposition of the examined aerosol drug in the lung in the function of inhalation time and peak inspiratory flow (Fig.1.), which could be a useful tool for the doctors in the selection of the appropriate inhalation drug, by knowing the correct inhalation parameters of the patient - these can help in elaboration of personalized treatment.

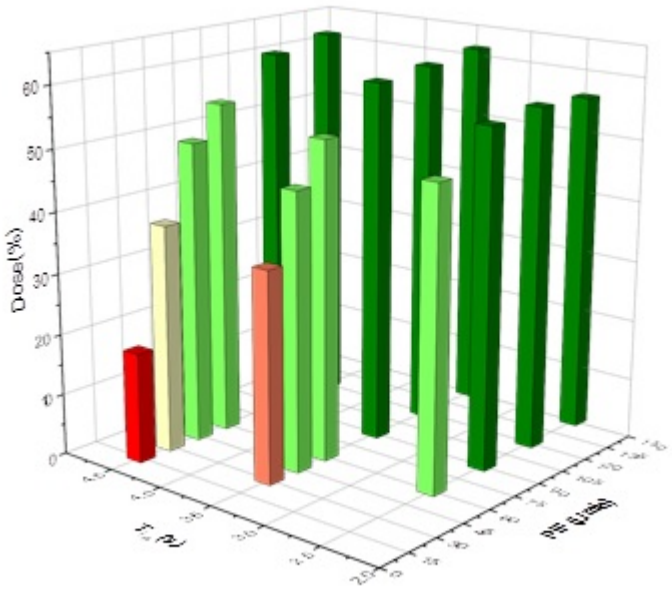

Figure 1. *The deposition efficiency map of a dry powder inhaler as a function of inhalation time (t_{in}) and peak inspiratory flow (PIF).*

Optical measurement techniques – We have been involved in the development of prototype instruments for medical surgery applications based on short pulse and fibre lasers. The light scattering and absorption properties of model tissue materials were studied using different lasers and detection techniques, as well as the aerosol plume that is generated upon the interaction of intense laser light and model tissue materials. The spreading, concentration and optical properties of the smoke was studied using high speed cameras and non-contact laser Doppler methods. We have been participating in the development of new technology based on 3D metal printing with industrial partners.

Our previously developed optical method was utilized in a research project aimed to investigate the properties of absorbing aerosols (mineral dust - black carbon mixtures) in the Mediterranean region. The main aims of the project are to characterize the aging and mixing of light-absorbing aerosol layers, to assess the contribution of individual aerosol components to the radiative forcing of mixed absorbing aerosol layers, to implement complex particle morphologies in radiative forcing estimates, and to investigate potential links between the presence of absorbing particles, aerosol layer lifetime and removal. Our instrument was installed into a research aircraft monitoring the vertical and horizontal profile of aerosol contamination of the atmosphere in given trajectories.

The development of light sources of our patented expanded beam imaging Spectro-ellipsometers are in progress in co-operation with the Centre for Energy Research, MFA. Bio-photonic research was conducted to optimize the label free, in-vivo fluorescence emission of different biological samples, according to their individual destruction thresholds, to develop an optimal excitation laser source.

2017

Aerosol drug delivery/deposition in human lungs. — The MMAD (mass median aerodynamic diameter) of the Symbicort® Turbuhaler dry powder inhaler (DPI) and the aerosol particle deposition in the upper airways was studied in case of different inhalation waveforms. For the detection of the aerosol size distribution, the Aerosol Particle Sizer (APS) Spectrometer was used. The effect of the breathing pattern on the MMAD was determined after the upper airways. With the help of the stochastic lung deposition model (SLDM), the amount of deposited particles in the lung was quantified. It was found that approximately 10% of the particles from the DPI deposit in the upper airways. The lung deposition of the drug from the DPI was calculated to be between 18 and 63% of the nominal dose, depending on the inhalation time and the peak inhalation flow.

Vibrational (Raman and infrared) spectroscopy based methods have been developed to determine the distribution of inhalation drugs (and other aerosols) in human airway replicas. The tested medication was introduced by metered dose inhaler into a realistic human lung tract prepared by 3D printing from computer tomographic data of human respiratory system. The deposited material was collected with silicon substrates attached to the hollow airway's walls in different points. The analysis of the substrates was performed by Raman and infrared spectroscopic mapping of drug's characteristic peak intensities over the surface. The method was verified by comparison with optical microscopic images recorded on the same surface area.

Study of optical properties of aerosols. — We have participated in the A-LIFE ERC project of the University of Vienna with PI Prof. Bernadett Weinzierl. The project is aimed at investigating the properties of absorbing aerosols (in particular mineral dust – black carbon (BC) mixtures) to characterize the aging and mixing of light-absorbing aerosol layers during their lifetime, to assess the contribution of individual aerosol components, in particular mineral dust and BC to the radiative forcing (RF) of mixed absorbing aerosol layers, to implement complex particle morphologies in RF estimates, and to investigate potential links between the presence of absorbing particles, aerosol layer lifetime and removal. We participated in the project by applying an optical method for the measurement of the optical and physical properties of ambient aerosols, which was developed by us in cooperation with the University of Vienna.

Optical thin film structures for advanced ultrafast applications. — We have continued our research concerning the development of optical thin film structures (high reflectors, output couplers, beam splitters, triple-band antireflective coatings etc.) for advanced femtosecond laser sources producing energetic light pulses in the near- and middle-infrared wavelength ranges. We have produced successfully sampling beam splitters on sapphire substrates for the French company Fastlite, working perfectly in their MIR laser system installed at ELI ALPS in Szeged already. We have developed new type of negative- or zero-dispersion multilayer mirror structures for our Japan partner also. The new laser mirror structures developed by us are very important in the development of new ultrafast high-power lasers which are able to shift the limits of the higher harmonic generation from the soft X-ray range to the hard X-ray range.

Optical measurement techniques serving the development of medical laser systems. — We have been involved in a project where the participants conduct research and development activities aiming at developing prototype instruments for medical surgery applications based on ultrashort pulse and fibre lasers. We have studied the light scattering and absorption properties of model tissue materials using different lasers and detection techniques. We have studied the surgical smoke that is generated upon the interaction of intense laser light and model tissue materials. In the frame of this study, we measured the size distribution of the surgical smoke with optical particle counter, aerodynamic particle counter and condensation particle counter, we measured the spread of the generated aerosols using laser Doppler anemometer, and collected samples with a cascade impactor for further analysis.